

# Selective Aerobic Oxidation of HMF to 2,5-Diformylfuran on Covalent Triazine Frameworks-Supported Ru Catalysts

Jens Artz,<sup>[a]</sup> Sabrina Mallmann,<sup>[b]</sup> and Regina Palkovits<sup>\*,[a]</sup>

The selective aerobic oxidation of 5-hydroxymethylfurfural (HMF) to 2,5-diformylfuran has been performed under mild conditions at 80 °C and 20 bar of synthetic air in methyl *t*-butyl ether. Ru clusters supported on covalent triazine frameworks (CTFs) allowed excellent selectivity and superior catalytic activity compared to other support materials such as activated carbon,  $\gamma$ -Al<sub>2</sub>O<sub>3</sub>, hydrotalcite, or MgO. CTFs with varying pore size, specific surface area, and N content could be prepared

from different monomers. The structural properties of the CTF materials influence the catalytic activity of Ru/CTF significantly in the aerobic oxidation of HMF, which emphasizes the superior activity of mesoporous CTFs. Recycling of the catalysts is challenging, but promising methods to maintain high catalytic activity were developed that facilitate only minor deactivation in five consecutive recycling experiments.

## Introduction

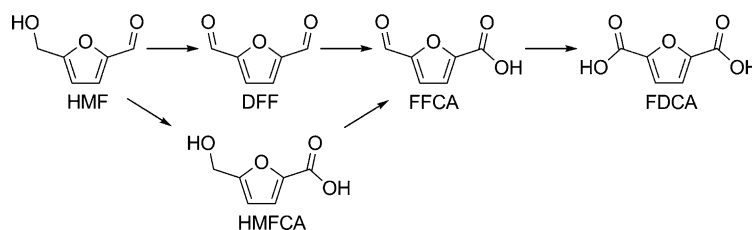
As fossil resources have been depleted drastically and energy consumption has increased rapidly during the last century, chemical processes independent of fossil resources have received growing attention in recent years. As a renewable carbon-containing resource, biomass has been the focus of numerous studies. The goal is to implement an environmentally benign continuous production of platform chemicals that does not depend on the diminishing fossil resources to enable sustainable industrial processes.<sup>[1,2]</sup> More recently, several attempts have been made to transform these biomass-derived platform chemicals selectively to highly valuable monomers, pharmaceuticals, and fine chemicals.<sup>[2]</sup>

5-Hydroxymethylfurfural (HMF) is a prominent biomass-derived platform chemical that can be obtained by the dehydration of hexoses such as glucose or fructose.<sup>[3,4]</sup> HMF can be hydrogenated to the corresponding diols, for example, 2,5-dihydroxymethyltetrahydrofuran,<sup>[5,6]</sup> used as a solvent or monomer,<sup>[6]</sup> or even 1,6-hexanediol, a monomer for the production of caprolactone.<sup>[7]</sup> Furthermore, several attempts have been made to oxidize HMF selectively to 2,5-diformylfuran (DFF) and 2,5-furandicarboxylic acid (FDCA).<sup>[8]</sup> Both are potential precursors for the poly-

mer industry. As an example, FDCA has been used successfully as a substitute for terephthalic acid in the production of polyethylene terephthalate (PET).<sup>[9]</sup>

DFF can be used as a precursor for pharmaceuticals, antifungal agents, furanic biopolymers, and furan-urea resins.<sup>[10-13]</sup> However, the selective oxidation of HMF to DFF is challenging because of the high reactivity of the aldehyde function. Therefore, DFF is transformed easily to 5-formyl-2-furancarboxylic acid (FFCA) and FDCA (Scheme 1). Additionally, the oxidation of HMF to the monocarboxylic acid 5-hydroxymethylfuran-2-carboxylic acid (HMFCa) can occur.

The methodology used most commonly to produce DFF selectively is the use of classical oxidants,<sup>[14]</sup> homogeneous Co



Scheme 1. Selective aerobic oxidation of HMF to DFF and its byproducts.

[a] J. Artz, Prof. Dr. R. Palkovits  
Chair of Heterogeneous Catalysis & Chemical Technology  
Institut für Technische und Makromolekulare Chemie  
RWTH Aachen University  
Worringerweg 1  
52074 Aachen (Germany)  
E-mail: palkovits@itmc.rwth-aachen.de

[b] S. Mallmann  
DWI Leibniz-Institut für Interaktive Materialien  
Forckenbeckstr. 50  
52074 Aachen (Germany)

Supporting Information for this article is available on the WWW under <http://dx.doi.org/10.1002/cssc.201403078>.

and Mn catalysts,<sup>[15]</sup> and V-based heterogeneous catalysts, such as V<sub>2</sub>O<sub>5</sub>/TiO<sub>2</sub> or vanadyl pyridine complexes supported on poly(vinylpyrrolidone) (PVP).<sup>[16]</sup> However, most of these catalysts suffer from low activities, high catalyst-to-substrate ratios and difficult recyclability because of their homogenous nature or the leaching of active species. Therefore, these systems are not suitable for sustainable DFF production.

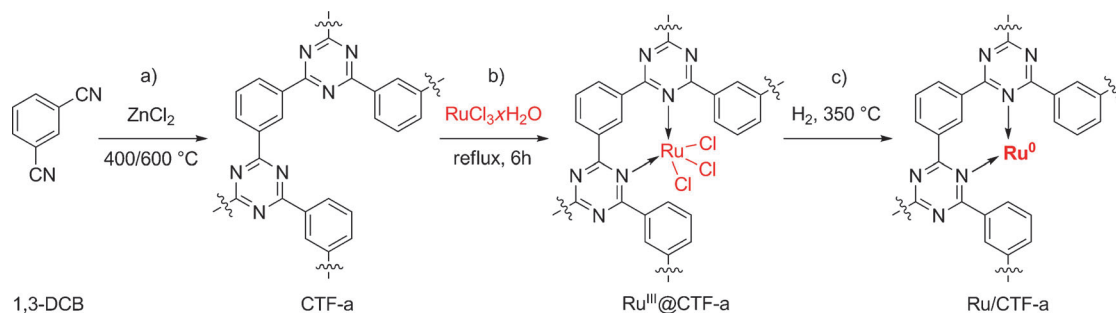
Recently, the first Ru-based solid catalysts have been reported for the oxidation of HMF to DFF. In 2011, Ebitani et al. showed that Ru on hydrotalcite can be used in the one-pot synthesis of DFF from glucose and fructose to yield 25 and

49% of DFF, respectively.<sup>[17]</sup> More recently the same group achieved DFF directly in a one-pot reaction from raffinose with 27% yield at 120 °C under a flow of O<sub>2</sub>. Antonyraj et al. achieved the full conversion of HMF with 97% selectivity to DFF at 130 °C and 2.8 bar O<sub>2</sub> after 4 h reaction time using Ru/γ-Al<sub>2</sub>O<sub>3</sub>.<sup>[18]</sup> Still, the conversion decreased over five consecutive recycling steps.

Nie et al. tested Ru on several supports at 110 °C with only a slight decrease in selectivity (96.2%) and activity over five cycles for Ru/C, which is the best catalyst to date.<sup>[19]</sup> However, the catalyst had to be reactivated by hydrothermal treatment for 4 h after each reaction cycle. They also showed that Ru/C was much more active than Pt, Pd, Rh, and Au-based catalysts. Moreover, a pressure of 20 bar of pure O<sub>2</sub> was necessary to achieve these results.

Zhang et al. used Co-Ce-Ru to reach an 82.6% DFF yield with 96.5% conversion after 12 h at 120 °C and only an atmospheric pressure of oxygen.<sup>[20]</sup> Furthermore, they enhanced the catalyst recycling by using magnetic separation with a Fe<sub>3</sub>O<sub>4</sub>@SiO<sub>2</sub>-NH<sub>2</sub>-Ru<sup>III</sup> catalyst, which attained 86.4% yield at full conversion after 4 h at 120 °C. Additionally, they used air at atmospheric pressure, which led to the same results but required prolonged reaction times of 16 h.

Herein, we present a versatile method for the preparation of nanoparticulate Ru catalysts stabilized on covalent triazine frameworks (CTF), a class of highly stable polymers formed by the trimerization of aromatic dinitriles in molten ZnCl<sub>2</sub>.<sup>[21]</sup> These materials are temperature stable up to 400 °C and insoluble in most common solvents. As a result of their desirable physical properties, CTFs meet the modern demands placed upon a solid catalyst suitable for use in sustainable chemistry.<sup>[22]</sup> We used various dinitrile monomers to access porous CTF materials that contain numerous N moieties, which allow the coordination of different molecular catalysts before reduction (Scheme 2). This approach allows both a molecular dispersion of metal species on the solid support<sup>[23]</sup> and a narrow particle size distribution of the metal nanoparticles formed upon reduction. Following this methodology, Ru/CTF materials were accessed that show high activity and selectivity in the aerobic oxidation of HMF to DFF even at low temperatures using synthetic air as the oxidant.

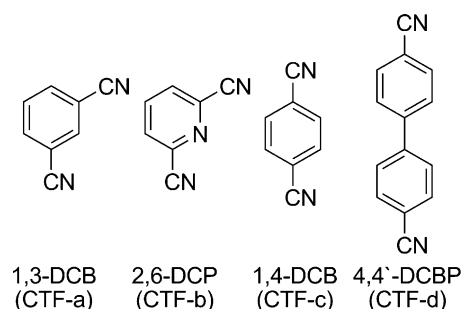


**Scheme 2.** a) Idealized synthesis of a CTF based on 1,3-DCB as a monomer (CTF-a). b) Proposed coordination approach of RuCl<sub>3</sub>·xH<sub>2</sub>O to form immobilized Ru<sup>III</sup>@CTF-a. c) Proposed stabilized metal nanoparticles after reduction in the presence of pure H<sub>2</sub>.

## Results and Discussion

### Catalyst preparation

We used 1,3-dicyanobenzene (1,3-DCB), 2,6-pyridinedicarbonitrile (2,6-DCP), 1,4-dicyanobenzene (1,4-DCB), and 4,4'-biphenyldicarbonitrile (4,4'-DCBP) as monomers to obtain CTF materials that contained numerous N moieties with different properties such as specific surface area, pore size and structure, and N content (Scheme 3). All these materials were synthesized



**Scheme 3.** Monomers applied as linkers in CTF synthesis.

using molten ZnCl<sub>2</sub> as the solvent in a ZnCl<sub>2</sub>/monomer molar ratio of 5:1. Heating the monomer/salt mixture to 400 °C and subsequently to 600 °C for at least 10 h each leads to the formation of a fully amorphous black solid with an extremely high surface area and bimodal micro- and mesoporosity. However, if the temperature was increased to 600 °C, partial carbonization is observed, which leads to decreased N contents compared to the applied monomer. This effect is especially visible for prolonged reaction times at 600 °C as the N content further decreases. Still, the number of N moieties is sufficient to enable the immobilization of homogeneous Ru precursors as will be discussed later. The N contents, specific surface areas, pore volumes, and the amounts of stabilized Ru in the prepared catalysts are summarized in Table 1. N<sub>2</sub> physisorption isotherms for all materials studied in this work are illustrated in Figure 1.

N<sub>2</sub> physisorption isotherms of all CTF polymers based on 1,3-DCB (CTF-a) correspond to type IV isotherms typical of

**Table 1.** Elemental analysis, specific surface area, total and micropore volume of monomers and CTF materials as well as Ru-content of the metal loaded Ru/CTF catalysts.

Monomer/ material	N <sup>[a]</sup> [%]	S <sub>BET</sub> <sup>[b]</sup> [m <sup>2</sup> g <sup>-1</sup> ]	V <sub>P(total)</sub> <sup>[c]</sup> [cm <sup>3</sup> g <sup>-1</sup> ]	V <sub>P(micro)</sub> <sup>[d]</sup> [cm <sup>3</sup> g <sup>-1</sup> ]	Ru <sup>[e]</sup> [%]
1,3-DCB	21.9 <sup>[g]</sup>	–	–	–	–
CTF-a	9.5	2439	1.96	0.47	4.32
CTF-a (20/20) <sup>[f]</sup>	11.1	2342	1.65	0.45	3.71
CTF-a (30/30) <sup>[f]</sup>	10.1	2255	1.56	0.42	3.38
CTF-a (40/40) <sup>[f]</sup>	9.3	2045	1.45	0.34	3.71
2,6-DCP	32.5 <sup>[g]</sup>	–	–	–	–
CTF-b	17.2	1179	0.64	0.64	3.34
1,4-DCB	21.9 <sup>[g]</sup>	–	–	–	–
CTF-c	10.4	2071	1.36	0.43	3.91
4,4'-DCBP	13.7 <sup>[g]</sup>	–	–	–	–
CTF-d	3.7	1683	2.63	0.30	3.99
Ru/C <sup>[h]</sup>	–	900	–	–	5.00
HT	–	8	0.2	0.2	6.08
MgO	–	60	–	–	6.58

[a] Determined by elemental analysis. [b] Surface area identified using the BET method. [c] Total pore volume determined at  $p/p_0 = 0.98$ . [d] Micropore volume calculated by N<sub>2</sub>-DFT model. [e] Determined by ICP-OES analysis after immobilization and reduction of the RuCl<sub>3</sub>·xH<sub>2</sub>O precursor under H<sub>2</sub> atmosphere, 3 h, 350 °C. [f] CTF-a X/Y was synthesized for X hours at 400 °C and further Y hours at 600 °C. [g] Theoretical value for N content; [h] Data provided by Sigma-Aldrich.

mesoporous materials (Figure 1 a). Prolonged synthesis times lead to a decrease in N<sub>2</sub> uptake and smaller hysteresis, which can be correlated with a decrease in specific surface areas (S<sub>BET</sub>) as well as total and micropore volumes. The structural parameters of the CTF materials can be controlled by varying the monomer. The CTF based on 2,6-DCP (CTF-b, Figure 1 b) exhibits a type I isotherm characteristic of microporous materials. This effect is most probably caused by a stable coordination of the pyridinic structure element of the monomer to the Lewis acidic ZnCl<sub>2</sub> during synthesis, which leads to a more dense coordination geometry during polymerization.<sup>[21b]</sup> The S<sub>BET</sub> and micropore volume of CTF-b are rather small compared to that of CTF-a. Nevertheless, because of the pyridine linkers, it contains a significantly higher amount of N compared to the other CTF materials. The N<sub>2</sub> physisorption isotherm of CTF-c (based on *para*-substituted 1,4-DCB) corresponds to a type IV isotherm, which emphasizes the mesoporous structure of the material. Interestingly, the amount of N<sub>2</sub> adsorbed and the hysteresis are much less pronounced according to the significantly lower S<sub>BET</sub> and pore volume values of CTF-c than that of CTF-a. The N content is comparable to that of CTF-a, as expected from the theoretical data for the monomers. CTF-d based on 4,4'-DCBP presents a highly mesoporous material with a moderate surface area of 1683 m<sup>2</sup> g<sup>-1</sup>. However, because of the low N content of its monomer, CTF-d exhibits a low number of coordination sites.

All of the prepared CTF materials show a comparable uptake of Ru during metal coordination followed by reduction under a H<sub>2</sub> atmosphere. The coordination mode adopted by Ru in these Ru<sup>III</sup>@CTF systems before reduction has not yet been identified completely. Future studies will focus on a compre-

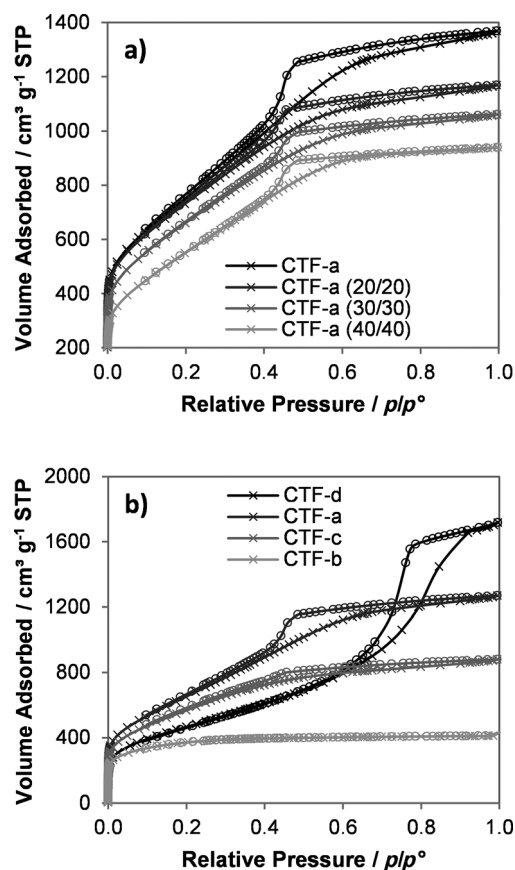


**Figure 1.** a) N<sub>2</sub> physisorption of CTF-a materials after different synthesis times denoted as CTF-a (X/Y) for synthesis for X h at 400 °C and Y h at 600 °C; (offset for CTF-a and CTF-a (20/20): +100 cm<sup>3</sup> g<sup>-1</sup>; offset for CTF-a (30/30): +50 cm<sup>3</sup> g<sup>-1</sup>) and b) N<sub>2</sub> physisorption of different CTF materials based on various linker molecules after synthesis for 10 h at 400 °C and 10 h at 600 °C.

hensive characterization of the interaction of metal species with these N-rich support materials. However, SEM with energy-dispersive X-ray spectroscopy (EDX) mapping demonstrates that Ru is dispersed finely throughout the support upon reduction to the nanoparticulate state (Figure 3). Furthermore, TEM images indicate that neither metal nanoparticles nor agglomerates are formed during coordination. Even after reduction to Ru<sup>0</sup> species, no nanoparticle formation could be observed by TEM, which indicates a high metal dispersion (Figure 2). In line with this, powder XRD patterns of the catalysts show no reflections of Ru<sup>0</sup> nanoparticles formed after re-

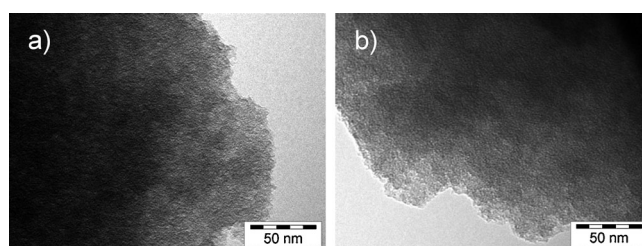


**Figure 2.** TEM images of a) Ru<sup>III</sup>@CTF-a and b) Ru<sup>0</sup>@CTF-a.

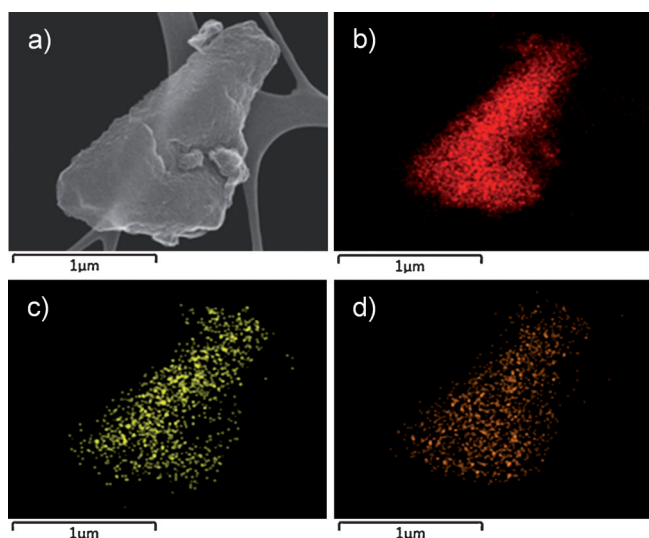


**Figure 3.** SEM/EDX mapping images of Ru/CTF-a. a) SEM of Ru/CTF-a. b) C mapping. c) N mapping. d) Ru mapping. Chloride was present throughout the whole sample, which indicates that Ru<sup>III</sup> species were not reduced fully to Ru<sup>0</sup> species.

duction of the coordinated complexes at 350 °C under a H<sub>2</sub> atmosphere. Clearly, Ru nanoparticles formed upon reduction are small and, therefore, X-ray amorphous, which confirms the efficient pre-coordination and stabilization on the N functionalities of the CTF supports. Comparable effects of N-containing support materials have been reported previously, for example, for Pd nanoparticles supported on comparable triazine frameworks as well as for Ru nanoparticles on N-functionalized carbon nanofibers.<sup>[24,25]</sup>

### Catalytic oxidation of HMF to DFF

Initially, the dependence of the catalytic activity of commercial Ru/C on different parameters and solvents was examined. Solvent screening showed that methyl *t*-butyl ether (MTBE) is the most appropriate solvent for both high catalytic activity and product separation (Table 2). As a result of its low

Table 2. Dependence of the catalytic activity on the solvent using Ru/C as a catalyst. <sup>[a]</sup>			
Solvent	Conversion <sup>[b]</sup> [%]	DFF yield <sup>[b]</sup> [%]	C balance <sup>[b]</sup> [%]
toluene	54.1	31.4	77.3
MTBE	54.5	43.7	89.2
1,4-dioxane	49.4	36.9	87.5
DMSO <sup>[c]</sup>	41.9	10.3	68.4
H <sub>2</sub> O <sup>[c]</sup>	55.1	28.9	73.8
acetone	47.9	37.0	89.1
acetonitrile	49.5	38.2	88.7

[a] Reaction conditions: 1 h, 80 °C, 20 bar of air, 15 mL solvent, 500 rpm stirring speed, HMF/metal molar ratio 40:1. [b] Determined by HPLC analysis. [c] In the presence of water, oxidation to FFCA takes place; hygroscopic DMSO seems to contain traces of water, which explains the lower selectivity to DFF.

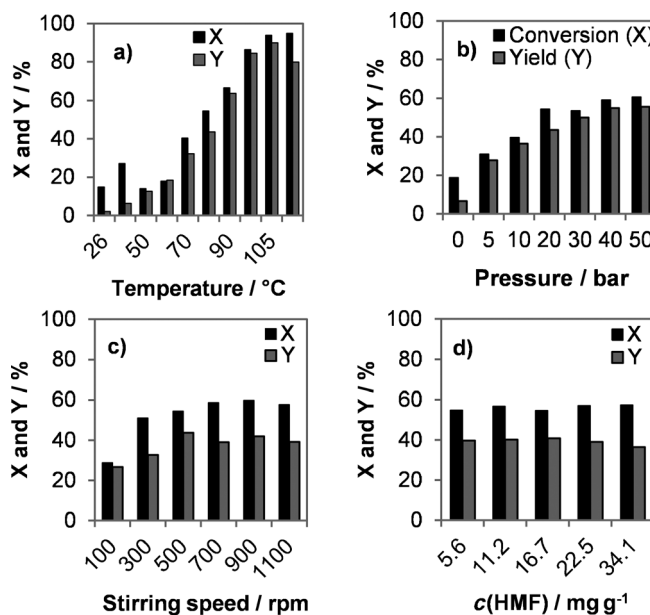


**Figure 4.** Dependence of the catalytic conversion on various parameters such as a) temperature, b) initial pressure of air, c) stirring speed, and d) HMF concentration in MTBE. Only one parameter was changed at a time and the others were maintained as follows. Reaction conditions: 1 h, 80 °C, 20 bar of air, 15 mL MTBE, 500 rpm stirring speed, Ru/C, HMF/metal molar ratio 40:1.

boiling point, MTBE is easily separated from the product at low temperature, and the conversion and yield were highest among the used solvents. The use of DMSO or water as the solvent led to lower yields of DFF caused by overoxidation to FFCA. Therefore, subsequent experiments to determine the influence of various reaction parameters were performed in MTBE (Figure 4).

Close to full conversion could be attained after 1 h at 110 °C and an initial pressure of 20 bar of synthetic air. Nevertheless, at 110 °C the yield of DFF decreases slightly. An explanation could be polymerization reactions of the product that already take place at these elevated temperatures. To study the influence of the different support materials presented in this work, reactions were performed at 80 °C to allow a moderate conversion of 54.5% of HMF with a DFF yield of 43.7% for commercial Ru/C. We varied the initial pressure of synthetic air to confirm minor changes of conversion and yield for pressures above 40 bar (Figure 4). The stirring speed does not have a great influence on the catalytic activity above 500 rpm. Furthermore, the HMF concentration in solution does not influence the catalytic conversion and DFF yield drastically as long as a molar ratio of 40:1 of HMF to the catalyst remains constant. This circumstance grants the use of concentrated solutions, reduces solvent needs, and enables easy and cost-efficient separation of the product, and the efficiency of the transformation of HMF into DFF is not affected.

With this in mind, catalytic test reactions for several catalyst supports were performed under optimized conditions for 1 h at 80 °C and 20 bar of air using MTBE as the solvent at 500 rpm stirring speed. No DFF formation occurred without catalyst. Both Pd/C and Pt/C resulted in poor DFF yields com-

Entry	Catalyst	Conversion <sup>[b]</sup> [%]	DFF yield <sup>[b]</sup> [%]	C balance <sup>[b]</sup> [%]
1	blank	8.3	0.1	91.8
2	Pd/C	19.4	8.8	89.4
3	Pt/C	28.5	1.3	72.8
4	Ru/C	54.5	43.7	89.2
5	Ru <sub>ox</sub> /C	30.9	11.4	80.5
6	Ru/ $\gamma$ -Al <sub>2</sub> O <sub>3</sub>	51.2	38.9	87.7
7	Ru/HT	15.3	1.0	85.7
8	Ru/MgO	15.8	1.6	85.8
9	Ru/CTF-a	86.3	63.6	77.3
10	Ru/C (RT) <sup>[c]</sup>	14.8	2.1	87.3
11	CTF-a	21.7	1.0	79.3

[a] Reaction conditions: 1 h, 80 °C, 20 bar of air, 15 mL MTBE, 500 rpm stirring speed, HMF/metal molar ratio 40:1. [b] Determined by HPLC analysis. [c] Adsorption test at RT, 500 rpm, atmospheric pressure.

pared to most of the Ru-based catalysts (Table 3, entries 2 and 3). Previous studies on Ru-based catalysts for the oxidation of HMF to DFF suggest Ru<sup>0</sup> as the active species. To support this hypothesis, Ru/C was calcined for 4 h at 300 °C under an air flow to form Ru<sub>ox</sub>/C. This catalyst enabled only 30.9% conversion and a significantly lower DFF yield of 11.4% compared to 43.7% for Ru<sup>0</sup>/C under the same conditions (Table 3, entry 4 vs. 5), which indicates the superior activity of reduced Ru catalysts. Nevertheless, a comprehensive investigation of the nature of the catalytically active sites is certainly necessary and will be targeted in future studies. Commercially available Ru/ $\gamma$ -Al<sub>2</sub>O<sub>3</sub> exhibited comparable conversions and DFF yields to Ru/C. In contrast, freshly prepared Ru catalysts on hydrotalcite (HT) and MgO with a rather high metal loading of 6.1 wt% for Ru/HT and 6.6 wt% for Ru/MgO were nearly inactive and resulted in poor yields of DFF (Table 3, entries 6–8). A reason for this might be the low specific surface area of both supports compared to all the other catalysts included in this study.

The most active catalyst, Ru/CTF-a, was prepared by reduction under H<sub>2</sub> atmosphere (Table 3, entry 9). Notably, for both Ru/CTF-a and Ru/C, DFF was the major product and only trace amounts of FFCA were observed. Nevertheless, in all experiments mass balances are not closed. Previous studies have shown that HMF is adsorbed strongly on the surface of different solid supports<sup>[26]</sup> and oligomeric byproducts<sup>[27]</sup> can be formed. Experiments with Ru/C at room temperature and only CTF-a under the standard reaction conditions were conducted (Table 3, entries 10 and 11). These experiments confirm that HMF consumption occurs even at room temperature and in the absence of a catalytically active species. At the same time no DFF is formed, which supports HMF adsorption as the origin for the gaps in the mass balances.

The dependence of the activity of several Ru catalysts supported on CTF materials on the material precursor and the synthesis conditions was investigated (Figure 5). Interestingly, HMF conversion and DFF yield can be correlated with porosity and specific surface area of the support material. In line, the maximum conversion could be achieved for Ru supported on

CTF-a, a support with a superior specific surface area and a moderate total pore volume (Table 1). Ru supported on microporous CTF-b, which has a significantly lower specific surface area, was nearly inactive, whereas Ru/CTF-c shows comparable results to Ru/CTF-a because of the comparable structural properties of these support materials. For Ru supported on CTF-d, a mesoporous support with a remarkably high total pore volume but only moderate specific surface area, a lower conversion was observed. Consequently, a high specific surface area of the support material seems to be essential for high catalytic activity. Furthermore, mesoporosity is advantageous for high catalytic activity compared to purely microporous support materials.

A similar trend can be observed for a single CTF material by varying the synthesis parameters to alter the structural parameters. The specific surface area and total pore volume of CTF-a decrease with prolonged synthesis times (Table 1). Accordingly, conversion and DFF yields decrease (Figure 5 b). For sub-

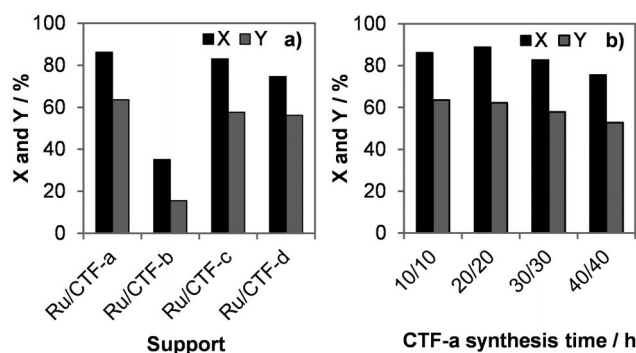


**Figure 5.** Dependence of the catalytic conversion (X: conversion; Y: yield) on the CTF support material. a) CTFs based on different monomers. b) CTF-a synthesized in various reaction times (X/Y). Reaction conditions: 1 h, 80 °C, 20 bar of air, 15 mL MTBE, 500 rpm stirring speed, HMF/metal molar ratio 40:1.

sequent investigations, CTF-a synthesized with 10 h time intervals was utilized, which reduced the overall synthesis time as well as the energy demand during synthesis.

To compare the catalytic performance of Ru/CTF-a to commercial Ru/C, time-resolved measurements were conducted (Figure 6). A certain conversion occurs during the heating of

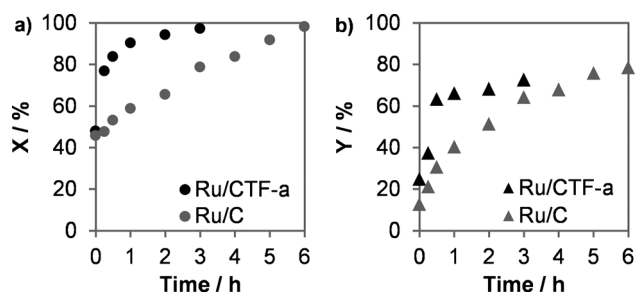


**Figure 6.** Time-resolved a) conversion (X) and b) DFF yield (Y) using Ru/CTF-a (black) and Ru/C (gray). Reaction conditions: 80 °C, 20 bar of air, 15 mL MTBE, 500 rpm stirring speed, HMF/metal molar ratio 40:1.

the autoclave to the desired temperature of 80 °C in approximately 10 min. Surprisingly, full conversion is already achieved after 3 h for Ru/CTF-a. In contrast, 6 h is required until full conversion with Ru/C. At approximately 84% conversion, Ru/CTF-a achieves a productivity of  $25.4 \times 10^{-3} \text{ mol g}^{-1} \text{ h}^{-1}$ , which is approximately seven times higher than the productivity of  $3.3 \times 10^{-3} \text{ mol g}^{-1} \text{ h}^{-1}$  for Ru/C. DFF yields remain limited to approximately 78%, which corresponds to our earlier observations. As no significant byproduct formation occurred and the reaction solutions remained colorless, we suggest the adsorption of HMF and DFF on the catalyst surface. Nevertheless, the formation of polymeric byproducts that adsorb on the catalysts cannot be excluded. For further comparison, the effect of the temperature on the activity and selectivity has been studied for Ru/CTF-a. After 1 h at 90 °C, a conversion of 92.3% and a 73.4% DFF yield were obtained. A further increase of the temperature to 100 °C led to 99.2% conversion and 77.9% DFF yield. Interestingly, after washing the catalyst with 15 mL of acetone and considering the extracted compounds in the mass balance, DFF yields could be further increased to 86.8% (90 °C, conversion ( $X$ ) = 90.5%) and 92.0% (100 °C,  $X$  = 99.1%), which leads to a nearly closed mass balance. This gives further evidence for the strong adsorption of both product and substrate as suggested before. At the same time, the conversion decreases slightly, as both DFF and HMF are adsorbed on the catalyst surface.

Ru/CTF-a and Ru/C have been recycled to investigate their stability (Figure 7). Both catalysts showed a strong loss in activity if simply washed with an organic solvent, dried under

active species into solution. The conversion did not increase if the filtered reaction mixture was used under the reaction conditions. Nevertheless, the current reactivation procedure relies on rather harsh conditions. The agglomeration of metal nanoparticles together with an associated loss of external metal surface area could cause the observed decrease in conversion and DFF yield. Furthermore, N<sub>2</sub> physisorption studies on the Ru/CTF-a catalyst as prepared and after five cycles reveal a significant loss of pore volume and surface area (Figure S1 and Table S1). This effect emphasizes a strong substrate and product adsorption as mentioned previously together with potential polymer formation. Consequently, further optimization of catalyst preparation and regeneration has to aim for reduced adsorption properties and suitable means to facilitate the complete removal of polymeric deposits. Therefore, future studies will aim to optimize recycling and reactivation conditions together with a continuous operation for HMF oxidation.

## Conclusions

An efficient catalyst system based on Ru supported on covalent triazine frameworks (CTFs) was developed for the selective oxidation of 5-hydroxymethylfurfural (HMF) to 2,5-diformylfuran (DFF) under aerobic conditions. The bimodal and mesoporous Ru/CTF catalysts showed high conversions and DFF yields at low temperatures using air as the sole oxidant and methyl *t*-butyl ether as an easily separable and reusable solvent. The catalytic activity depends strongly on the structural parameters of the CTF materials, such as specific surface area and total pore volume. These parameters can be controlled by the choice of the linker as well as the synthesis time for the framework. High conversions of 97.3% and DFF yields of 72.7% could be obtained after only 3 h at 80 °C using 20 bar of air. At 84% HMF conversion, the productivity of Ru/CTF-a was nearly seven times higher than that of Ru/C. The recycling of these Ru-based catalysts is still challenging. Nevertheless, Ru/CTF-a exhibits only minor deactivation if a reactivation procedure is applied under H<sub>2</sub> flow. Therefore, this concept paves the way for an environmentally benign continuous production of biomass-derived chemicals that does not depend on diminishing fossil resources and enables sustainable industrial processing.

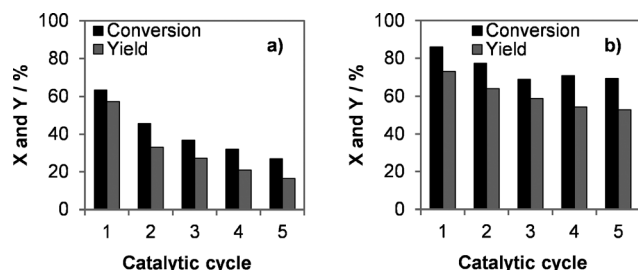


**Figure 7.** Recycling study of a) Ru/C and b) Ru/CTF-a. Reaction conditions: 1 h, 80 °C, 20 bar of air, 15 mL MTBE, 500 rpm stirring speed, HMF/metal molar ratio 40:1. Catalysts were reactivated after each run.

vacuum, and reused without further treatment. Our findings suggest that not only polymeric surface species but also the surface oxidation of the supported metal nanoparticles cause the observed loss of activity. Therefore, catalysts were reactivated at 350 °C for 3 h under H<sub>2</sub> flow. With this strategy, a significantly reduced deactivation could be achieved together with the stable catalytic activity of Ru/CTF-a after two recycling steps. Overall, Ru/CTF-a exhibits not only superior activity but also minor deactivation compared to Ru/C. We assign this observation to the N functionalities of the support that provide a stabilizing effect to the Ru species and hinder agglomeration and leaching of metal species.<sup>[24,25]</sup> Additionally, hot filtration tests were performed to exclude the leaching of catalytically

## Experimental Section

### Catalyst preparation

For the synthesis of CTF-a, 1,3-dicyanobenzene (0.621 g, 4.85 mmol, 1 equiv.) and ZnCl<sub>2</sub> (3.305 g, 24.25 mmol, 5 equiv.) were mixed and ground together, transferred into a quartz ampoule, and dried under vacuum for at least 3 h. The ampoule was then flame-sealed and placed inside a furnace for 10 h of heat treatment at 400 °C and a further 10 h at 600 °C (heating rate: 10 Kmin<sup>-1</sup>). After cooling to RT, the ampoule was broken open (CAUTION: the ampoules are under pressure, which is released during opening), and the solid product was ground and washed thoroughly with water and dilute HCl (0.1 M). The solid material was then ground in a ball mill (Fritsch Pulverisette23, 5 min, 30 Hz) to obtain a black powder, which was washed successively with water, dilute HCl,

dilute NaOH, water, and THF and dried under vacuum for at least 12 h. Materials based on 2,6-pyridinedicarbonitrile (CTF-b), 1,4-dicyanobenzene (CTF-c), and 4,4'-biphenyldicarbonitrile (CTF-d) were synthesized as described for 1,3-DCB. For Ru impregnation, CTF (600 mg) was added to a solution of  $\text{RuCl}_3 \cdot x\text{H}_2\text{O}$  (0.079 g, 0.381 mmol) in EtOH (400 mL) that was heated to reflux and stirred for 6 h. After cooling to RT, the  $\text{Ru}^{\text{III}}\text{@CTF}$  material was collected by filtration and washed with EtOH to remove uncoordinated Ru precursor. After drying under vacuum at 60 °C for at least 12 h, the  $\text{Ru}^{\text{III}}\text{@CTF}$  material was reduced in a tube furnace under a  $\text{H}_2$  atmosphere (heating rate: 10  $\text{K min}^{-1}$ , 350 °C,  $\text{H}_2$  flow 100  $\text{mL min}^{-1}$ , 3 h) to obtain Ru/CTF (for Ru loading, see Table 1). Ru/C, Ru/ $\gamma$ - $\text{Al}_2\text{O}_3$ , Pd/C, and Pt/C catalysts (5 wt%) were purchased from Sigma Aldrich and were used as received. Ru/HT (HT composition:  $\text{CH}_{16}\text{Al}_2\text{Mg}_6\text{O}_{19} \cdot 4\text{H}_2\text{O}$ ) and Ru/MgO were prepared by wet impregnation from  $\text{RuCl}_3 \cdot x\text{H}_2\text{O}$  (0.1313 g, 0.633 mmol) in EtOH (20 mL) with the particular support (1.0 g). All supported metal precursors were reduced using the method described for  $\text{Ru}^{\text{III}}\text{@CTF}$ . The CTF materials were characterized by thermogravimetric analysis (TGA), elemental analysis,  $\text{N}_2$  sorption measurements, TEM, and XRD. The Ru-doped materials were analyzed using inductively coupled plasma optical emission spectroscopy (ICP-OES), SEM/EDX, TEM, and XRD.

### Selective oxidation of HMF to DFF

Typically, a stainless-steel autoclave (75 mL) with a glass inlet was charged with a solution of HMF (0.1261 g, 1 mmol) in solvent (15 mL). The catalyst (HMF/metal molar ratio: 40:1) was added, and the autoclave was equipped with a stirring bar and temperature sensor. It was sealed, pressurized to 20 bar with synthetic air (hydrocarbon free), and heated to 80 °C with stirring at 500 rpm. After a certain time, the autoclave was cooled and depressurized. The catalyst was removed by filtration with a syringe filter (CHROMAFIL Xtra, PA-20/25, 0.20  $\mu\text{m}$ ), and the reaction solution was analyzed by HPLC (Shimadzu 2020, 300  $\times$  8.0 mm organic acid resin column,  $T=40$  °C, UV detector at  $\lambda=254$  nm for HMF and DFF, refractive index detector (RID-10A) detector for HMFCA, FFCA, and FDCA) with 154  $\mu\text{L}$  trifluoroacetic acid in 1 L water as an eluent (flow rate: 1  $\text{mL min}^{-1}$ ). For recycling studies, the catalysts were collected by filtration by using a Whatman filtration system equipped with Anodisc 25 (0.20  $\mu\text{m}$ ) membranes, washed thoroughly with solvent, dried overnight under vacuum at 60 °C and reactivated in a tube furnace under a  $\text{H}_2$  atmosphere (10  $\text{K min}^{-1}$ , 350 °C,  $\text{H}_2$  flow 100  $\text{mL min}^{-1}$ , 3 h) to regain activity. Conversions (X) and yields (Y) were calculated as follows:  $X(\text{HMF}) = (n_0(\text{HMF}) - n_1(\text{HMF})) / n_0(\text{HMF}) \times 100\%$ , in which  $n_0$  is the initial molar amount of HMF and  $n_1$  is the molar amount of unreacted HMF, and  $Y(\text{DFF}) = n(\text{DFF}) / n_0(\text{HMF}) \times 100\%$  for the formation of one molecule of DFF per molecule of HMF.

### Acknowledgements

We acknowledge financial support from the DFG (PA1689/1-1) and funding from the Excellence Initiative of the German federal and state governments. SEM/EDX mapping was performed at the Center for Chemical Polymer Technology CPT, which is supported by the EU and the federal state of North Rhine-Westphalia (grant no. EFRE 30 00 883 02). We thank Mr. B. Spliethoff and Mr. A. Dreier for the TEM measurements, as well as the microanalytic

laboratory Kolbe (Mülheim an der Ruhr, Germany) for CHN analysis.

**Keywords:** biomass • heterogeneous catalysis • oxidation • ruthenium • supported catalysts

- [1] a) J. N. Chheda, G. W. Huber, J. A. Dumesic, *Angew. Chem. Int. Ed.* **2007**, *46*, 7164–7183; *Angew. Chem.* **2007**, *119*, 7298–7318; b) M. J. Climent, A. Corma, S. Iborra, *Green Chem.* **2011**, *13*, 520–540.
- [2] A. Corma, S. Iborra, A. Velty, *Chem. Rev.* **2007**, *107*, 2411–2502.
- [3] a) J. N. Chheda, Y. Román-Leshkov, J. A. Dumesic, *Green Chem.* **2007**, *9*, 342–350; b) H. Zhao, J. E. Holladay, H. Brown, Z. C. Zhang, *Science* **2007**, *316*, 1597–1600; c) I. Delidovich, K. Leonhard, R. Palkovits, *Energy Environ. Sci.* **2014**, *7*, 2803–2830.
- [4] a) A. A. Rosatella, S. P. Simeonov, R. F. M. Frade, C. A. M. Afonso, *Green Chem.* **2011**, *13*, 754–793; b) R.-J. van Putten, J. C. van der Waal, E. de Jong, C. B. Rasrendra, H. J. Heeres, J. G. de Vries, *Chem. Rev.* **2013**, *113*, 1499–1597.
- [5] R. Alamillo, M. Tucker, M. Chia, Y. Pagán-Torres, J. Dumesic, *Green Chem.* **2012**, *14*, 1413–1419.
- [6] a) A. J. Sanborn, P. D. Bloom, US Pat, **2008**, 7579490; b) C. Moreau, M. N. Belgacem, A. Gandini, *Top. Catal.* **2004**, *27*, 11–30.
- [7] T. Buntara, S. Noel, P. H. Phua, I. Melián-Cabrera, J. G. de Vries, H. J. Heeres, *Angew. Chem. Int. Ed.* **2011**, *50*, 7083–7087; *Angew. Chem.* **2011**, *123*, 7221–7225.
- [8] a) P. Verdegue, N. Merat, A. Gaset, *J. Mol. Catal.* **1993**, *85*, 327–344; b) C. Carlini, P. Patrono, A. M. R. Galletti, G. Sbrana, V. Zima, *Appl. Catal. A* **2005**, *289*, 197–204; c) A. S. Amarasekara, D. Green, E. McMillan, *Catal. Commun.* **2008**, *9*, 286–288; d) X. Xiang, L. He, Y. Yang, B. Guo, D. M. Tong, C. W. Hu, *Catal. Lett.* **2011**, *141*, 735–741.
- [9] a) A. Gandini, M. N. Belgacem, *Prog. Polym. Sci.* **1997**, *22*, 1203–1379; b) E. de Jong, A. Dam, L. Sipo, G.-J. M. Gruter in *Biobased Monomers, Polymers and Materials, Vol. 1105* (Eds.: P. B. Smith, R. A. Gross), American Chemical Society, Washington DC, **2012**, pp. 1–13; c) A. J. J. E. Eerhart, A. P. C. Faaij, M. K. Patel, *Energy Environ. Sci.* **2012**, *5*, 6407–6422.
- [10] K. T. Hopkins, W. D. Wilson, B. C. Bender, D. R. McCurdy, J. E. Hall, R. R. Tidwell, A. Kumar, M. Bajic, D. W. Boykin, *J. Med. Chem.* **1998**, *41*, 3872–3878.
- [11] M. Del Poeta, W. A. Schell, C. C. Dykstra, S. K. Jones, R. R. Tidwell, A. Kumar, D. W. Boykin, J. R. Perfect, *Antimicrob. Agents Chemother.* **1998**, *42*, 2503–2510.
- [12] A. Gandini, N. M. Belgacem, *Polym. Int.* **1998**, *47*, 267–276.
- [13] A. S. Amarasekara, D. Green, L. D. Williams, *Eur. Polym. J.* **2009**, *45*, 595–598.
- [14] L. Cottier, G. Descotes, E. Viollet, J. Lewkowski, R. Skowronski, *J. Heterocycl. Chem.* **1995**, *32*, 927–930.
- [15] W. Partenheimer, V. V. Grushin, *Adv. Synth. Catal.* **2001**, *343*, 102–111.
- [16] a) C. Moreau, R. Durand, C. Pourcheron, D. Tichit, *Stud. Surf. Sci. Catal.* **1997**, *108*, 399–406; b) O. C. Navarro, A. C. Canós, S. I. Chornet, *Top. Catal.* **2009**, *52*, 304–314.
- [17] a) A. Takagaki, M. Takahashi, S. Nishimura, K. Ebitani, *ACS Catal.* **2011**, *1*, 1562–1565; b) S. Dabral, S. Nishimura, K. Ebitani, *ChemSusChem* **2014**, *7*, 260–267.
- [18] C. A. Antonyraj, J. Jeong, B. Kim, S. Shin, S. Kim, K.-Y. Lee, J. K. Cho, *J. Ind. Eng. Chem.* **2013**, *19*, 1056–1059.
- [19] a) J. Nie, J. Xie, H. Liu, *J. Catal.* **2013**, *301*, 83–91; b) J. Nie, J. Xie, H. Liu, *Chin. J. Catal.* **2013**, *34*, 871–875.
- [20] a) Y. Wang, B. Liu, K. Huang, Z. Zhang, *Ind. Eng. Chem. Res.* **2014**, *53*, 1313–1319; b) S. Wang, Z. Zhang, B. Liu, J. Li, *Ind. Eng. Chem. Res.* **2014**, *53*, 5820–5827.
- [21] a) P. Kuhn, M. Antonietti, A. Thomas, *Angew. Chem. Int. Ed.* **2008**, *47*, 3450–3453; *Angew. Chem.* **2008**, *120*, 3499–3502; b) P. Kuhn, A. Thomas, M. Antonietti, *Macromolecules* **2009**, *42*, 319–326.
- [22] a) J. Roeser, K. Kailasam, A. Thomas, *ChemSusChem* **2012**, *5*, 1793–1799; b) P. Katekomol, J. Roeser, M. Bojdys, J. Weber, A. Thomas, *Chem. Mater.* **2013**, *25*, 1542–1548.
- [23] a) R. Palkovits, M. Antonietti, P. Kuhn, A. Thomas, F. Schüth, *Angew. Chem. Int. Ed.* **2009**, *48*, 6909–6912; *Angew. Chem.* **2009**, *121*, 7042–

- 7045; b) M. Soorholtz, R. J. White, T. Zimmermann, M.-M. Titirici, M. Antonietti, R. Palkovits, F. Schüth, *Chem. Commun.* **2013**, 49, 240–242.
- [24] C. E. Chan-Thaw, A. Villa, G. M. Veith, K. Kailasam, L. A. Adamczyk, R. R. Unocic, L. Prati, A. Thomas, *Chem. Asian J.* **2012**, 7, 387–393.
- [25] S. Armenise, L. Roldán, Y. Marco, A. Monzón, E. García-Bordejé, *J. Phys. Chem. C* **2012**, 116, 26385–26395.
- [26] C. Detoni, C. H. Gierlich, M. Rose, R. Palkovits, *ACS Sustainable Chem. Eng.* **2014**, 2, 2407–2415.
- [27] K. Pupovac, R. Palkovits, *ChemSusChem* **2013**, 6, 2103–2110.

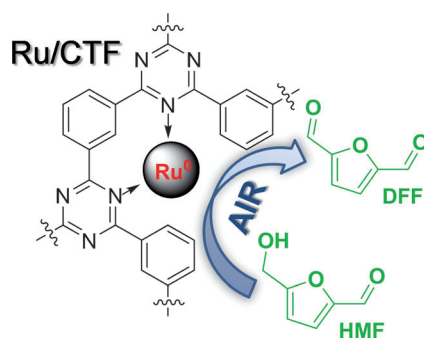
---

Received: October 2, 2014

Published online on ■ ■ ■■, 0000

## FULL PAPERS

**Oxidize and conquer:** 5-Hydroxymethylfurfural (HMF) has been oxidized selectively to 2,5-diformylfuran (DFF) using air under mild conditions with Ru supported on covalent triazine frameworks (CTFs) as catalysts. These catalysts result in higher conversions and yields compared to commercially available Ru/C and show superior stability in recycling studies.



*J. Artz, S. Mallmann, R. Palkovits\**

■■ - ■■

**Selective Aerobic Oxidation of HMF to 2,5-Diformylfuran on Covalent Triazine Frameworks-Supported Ru Catalysts**

